SUSX-TH-96-008
astro-ph/9606137

Correlations in Cosmic String Networks

Graham R. Vincent[(a)*]
Mark Hindmarsh[(a)†]
Mairi Sakellariadou[(b)‡]

February 5, 2008

[(a)] *School of Mathematical and Physical Sciences*
University of Sussex
Brighton BN1 9QH
UK

[(b)] *Département de Physique Théorique*
Université de Genève
Quai Ernest-Amsermet 24
CH-1211 Genève 4
Switzerland

Abstract

We investigate scaling and correlations of the energy and momentum in an evolving network of cosmic strings in Minkowski space. These quantities are of great interest, as they must be understood before accurate predictions for the power spectra of the perturbations in the matter and radiation in the early Universe can be made. We argue that Minkowski space provides a reasonable approximation to a Friedmann background for string dynamics and we use our results to construct a simple model of the network, in which it is considered to consist of randomly placed segments moving with random velocities. This model works well in accounting for features of the two-time correlation functions, and even better for the power spectra.

*E-mail: g.r.vincent@sussex.ac.uk
†E-mail: m.b.hindmarsh@sussex.ac.uk
‡E-mail: mairi@karystos.unige.ch

1 Introduction

Phase-ordering dynamics after a cosmological phase transition may explain the origin of structure in our universe [1]. Our interest is in the role of one class of theories - cosmic strings [2].

Recent attention has focused on cosmic strings formed during the breaking of the grand unified symmetry, which naturally generates perturbations in the matter and radiation fields of the right order for structure formation. However, to make diagnostic predictions between cosmic strings, other defects and inflation-based theories we need to use a detailed theory of the cosmological evolution of perturbations. There exists a well-founded theory for the standard inflationary scenario of gaussian fluctuations in the gravitational potential. In extending the theory to cover defect-based theories there are three principal issues to be faced. Firstly, although the initial conditions are random, they are not gaussian which makes averaging over the ensembles of defects a numerical problem. Secondly, the creation of the defects must conserve energy-momentum: hence there are compensating fluctuations in the fluid components on super-horizon scales. Thirdly, in the subsequent evolution, the defect stress-energy $\Theta_{\mu\nu}$ must be included in the Einstein equations. Defects form an unusual component of the total stress-energy, in that the metric perturbations only affect the evolution of the defect network to second order, so in the linear approximation we can evolve the network in the unperturbed background metric. Its stress-energy then acts as a source term for the familiar set of differential equations governing the evolution of the perturbations. As demonstrated by Veeraraghavan and Stebbins [3], the solutions to the Einstein equations describing the *subsequent* evolution of perturbation variables with a source term can be expressed as a convolution of a suitable Green's function (dependent on the usual cosmological parameters) with the source term integrated over time. For a set of perturbation variables Δ_a and a set of source terms S_b related to $\Theta_{\mu\nu}$

$$\Delta_a(k,\eta) = \int_{\eta_i}^{\eta} d\eta'\, G_{ab}(\eta,\eta') S_b(k,\eta') \tag{1}$$

where η and η' are conformal times and k is the wavenumber of the mode. Calculating the power in these variables will then involve integrating over the two-time correlator

$$\langle |\Delta_a(k,\eta)|^2 \rangle = \int_{\eta_i}^{\eta} d\eta'\, d\eta''\, G_{ab}(\eta,\eta') G_{ac}(\eta,\eta'') \langle S_b(k,\eta') S_c(k,\eta'') \rangle \tag{2}$$

When using the Veeraraghavan-Stebbins formalism, the Green's functions can be calculated from standard cosmological perturbation theory: analytically in the simplest cases, or numerically for a more realistic universe. However, in the absence of a workable ana-

lytic treatment of string evolution (although see [4] and [5]) we must rely for the moment on a numerical study of the two-time correlators.

In a simplified model the Universe consists of two fluids: a pressureless CDM component and a tightly-coupled baryon-photon fluid. In the convenient synchronous gauge, the sources are Θ_{00} and $i\hat{k}_j\Theta_{0j}$ (which we shall hereafter call U), when the equations are rewritten using the energy-momentum pseudotensor introduced by Veeraraghavan and Stebbins [3]. In the Newtonian gauge they are also the sources of curvature fluctuations [6]. It is therefore the two-time correlation functions of these variables that we study. Such a study is particularly timely in view of recent work on the power spectrum of Cosmic Microwave Background around the degree scale from strings [7, 8] and from global textures [9, 10]. As emphasised by Albrecht *et al* [11], the distinctive appearance of "Doppler" peaks and troughs seen in inflationary calculations and texture models depend sensitively on the temporal coherence of the sources. If one assumes little coherence the peaks are washed out; on the other hand an assumption of total coherence preserves them. Magueijo *et al* in [7] assumed that strings were effectively incoherent and obtained a rather featureless CMB power spectrum at large multipole l. In [8] this assumption was justified by a numerical study of the two-time energy-density correlator.

In contrast both Durrer *et al* [9] and Crittenden and Turok [10] assumed maximum coherence for their texture models and found that the peaks were preserved, albeit in positions typical of isocurvature models [6]. It is therefore clear that understanding the temporal coherence of string sources is of great importance when calculating their microwave background signals.

In this paper we present the results of some numerical "experiments" evolving strings in Minkowski space. Using Minkowski space rather than a Friedmann model may seem rather unrealistic. However, we expect a network of strings evolving in Minkowski space to have all the essential features of one in a Friedmann background. A tangled initial state consisting of a few probably "infinite" strings plus a scale free distribution of loops straightens out under tension and continually self intersects resulting in the transfer of energy into very small fast moving loops. The infinite string approaches "scaling" in which it is characterised as a set of more or less Brownian random walks. The step length of the walks and their average separation are both approximately equal to an overall network scale ξ, which increases linearly with time (as naive dimensional analysis would suggest). The length density of the infinite string decreases as ξ^{-2}, again as dimensional analysis suggests. In fact, ξ is conventionally defined so that the length density is precisely $1/\xi^2$ [12]. The effect of an expanding background is to damp coherent motions on super-horizon scales. However the network scale is much less that the horizon size so one can argue that the expansion does not significantly affect the network dynamics. The great

advantage of Minkowski space is that the network evolution is very easy to simulate numerically: the code is generally many times shorter than an equivalent code for a Friedmann background [13, 14], and makes fewer demands on both RAM and CPU time. We are therefore able to get much better statistical significance from the data.

We present results from an extensive programme of numerical simulations for the two-time correlators of Θ_{00} and U, and use a simple model to explain most of the features we observe. It turns out that, to a good approximation, the network can be thought of as consisting of randomly placed segments of string with random velocities. The segments are of length ξ and number density ξ^{-3}, thus reproducing the correct behaviour for the length density.

In this model it is easy to show that the coherence time-scale in a Fourier mode of wavenumber k is determined by the time segments take to travel a distance k^{-1}. The model in fact predicts that the correlations between the energy density at times η and η' decrease as $\exp(-\frac{1}{6}k^2\bar{v}^2(\eta-\eta')^2)$, where $\bar{v}$ is the r.m.s string velocity. Hence we can talk of a coherence time-scale $\eta_c = \sqrt{3}/\bar{v}k$, which is the time over which the correlation function falls to $e^{-\frac{1}{2}}$ of its equal time value. Given that we find $\bar{v}^2 = 0.36$, the model predicts $\eta_c \simeq 3/k$. Our results actually indicate that at high k, η_c decreases faster than k^{-1}, but we have some evidence that this behaviour is a lattice artifact.

2 Flat Space Strings

We use a development of a code written by one of us some time ago [15, 16]. Initial string realisations are generated using the Vachaspati-Vilenkin algorithm [17]. This mimics the Kibble mechanism for the spontaneous breaking of a scalar U(1) symmetry with a "Mexican hat" potential, as the Universe cools through a thermal phase transition.

This initial configuration is set up for evolution on a cubic lattice with fundamental lattice side δ. We are free to alter the initial correlation length ξ_0 in terms of δ and we may add structure to the network by placing a percentage P_c of cusps randomly along the string. Cusps are string links which are confined to one lattice site and which move at the speed of light. Adding cusps avoids peculiarities arising from having long straight segments of string in the initial conditions.

In Minkowski space the string equations of motion are

$$\mathbf{X}'' = \ddot{\mathbf{X}} \tag{3}$$

where $\dot{} = \partial/\partial\eta$ and $' = \partial/\partial\sigma$; η is time and σ is a space-like parameter along the string. If we regard Minkowski space as a Friedmann-Roberston-Walker Universe in the limit

that the expansion rate goes to zero, then η can be identified as FRW conformal time. $\mathbf{X} = \mathbf{X}(\sigma, \eta)$ is a position three-vector which satisfies

$$\mathbf{X}' \cdot \dot{\mathbf{X}} = 0 \tag{4}$$

$$\mathbf{X}'^2 + \dot{\mathbf{X}}^2 = 1 \tag{5}$$

This is a convenient set of constraints, as (5) ensures that the energy of a segment of string is proportional to its length in σ.

We solve this using the Smith-Vilenkin algorithm [18] which is based on the exact finite difference solution to (3),

$$\mathbf{X}(\sigma, \eta + \delta) = \mathbf{X}(\sigma + \delta, \eta) + \mathbf{X}(\sigma - \delta, \eta) - \mathbf{X}(\sigma, \eta - \delta) \tag{6}$$

If the string points are initially defined on the sites of a cubic lattice $(N\delta)^3$, then (6) ensures that they remain on the lattice at time steps of δ. One can see from (6) that stationary elementary segments have length (and hence energy) of 2δ and point in one of six directions.

Because the string points lie on the sites of the lattice, identifying crossing events is easy. When two strings cross, they intercommute with a probability which is set to 1. Loops with energy greater than or equal to a threshold value of E_c are allowed to leave the network, while reconnections are forbidden for loops with energy equal to E_c. Forbidding reconnections allows energy to leave the network fairly efficiently; otherwise it takes much longer for the effect of the initial conditions to wear off. The natural and usual value for E_c is the minimum segment length, 2δ. In fact, most of the energy in the string network goes into the smallest possible loops. In some sense, the cusps model the gravitational radiation of a realistic string network: They travel at the speed of light and do not subsequently interact with the network.

Each realisation is evolved on a $(64\delta)^3$ or a $(128\delta)^3$ lattice with approximately 7500 or 60000 points describing the string network. For calculating quantities like power spectra and two-time correlation functions we typically average over 50 realisations.

3 Results

The energy-momentum tensor for a cosmic string at a point $\mathbf{x}$ is

$$\Theta^{\mu\nu}(\mathbf{x}) = \int d\sigma (\dot{X}^\mu \dot{X}^\nu - X'^\mu X'^\nu) \delta^{(3)}(\mathbf{x} - \mathbf{X}(\sigma, \eta)) \tag{7}$$

It is simple to calculate this on a cubic lattice for our string realisations, and use a Fast Fourier Transform to get a Fourier mode representation. Here we want to measure the

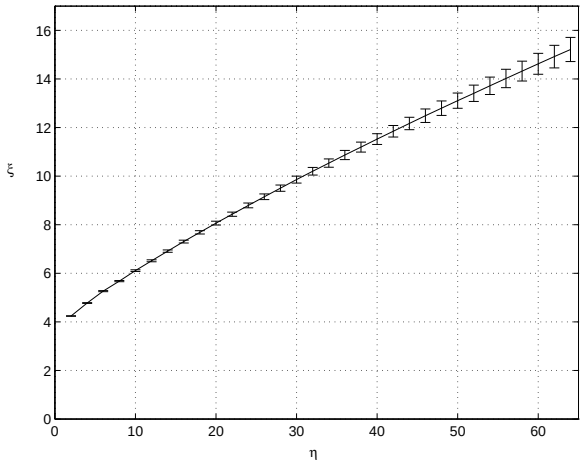

Figure 1: The energy-density length scale ξ over time η for a 128^3 lattice, averaged over 50 realisations

power spectra of $\Theta_{00}(k)$ and $U(k)$. These are calculated by averaging the amplitudes over all Fourier modes with a wavenumber between k and $k + 2\pi/\delta$.

Previous work [15, 16, 19] has tried to identify those features of the network that are scaling, when a relevant length scale grows with the horizon. For example, we can define the familiar energy density scale ξ by $\xi^2 = \mu/\rho_{\rm inf}$ where $\rho_{\rm inf}$ is the density of string with energy greater than ξ. (This apparently circular definition works because we know the initial step length ξ_0 and to calculate $\rho_{\rm inf}$ we use ξ from the previous time step). Scaling is reached when $x = \partial\xi/\partial\eta$ is constant. In the cases considered here $x = 0.15$ ($E_c = 2\delta$) and $x = 0.12$ ($E_c = 4\delta$). The usual definition for scaling, that $x = \xi/\eta$ is constant, can not be used here as throughout our simulations ξ_0 is too large to be ignored. For this reason, we express all scaling functions in terms of ξ, rather than η. The behaviour of ξ is shown in Figure 1.

The infinite string energy-momentum power spectra also exhibit scaling behaviour, which we express in terms of the scaling functions P^ρ and P^U. We also consider the equal time cross correlation function $\langle U(k)\Theta^*_{00}(k)\rangle$ which is a real function within the ensemble errors.

$$\langle|\Theta_{00}(k,\eta)|^2\rangle = \frac{VP^\rho(k\xi)}{\xi} \tag{8}$$

$$\langle U(k)\Theta^*_{00}(k)\rangle = \frac{VX^{\rho U}(k\xi)}{\xi} \tag{9}$$

$$\langle|U(k,\eta)|^2\rangle = \frac{VP^U(k\xi)}{\xi} \tag{10}$$

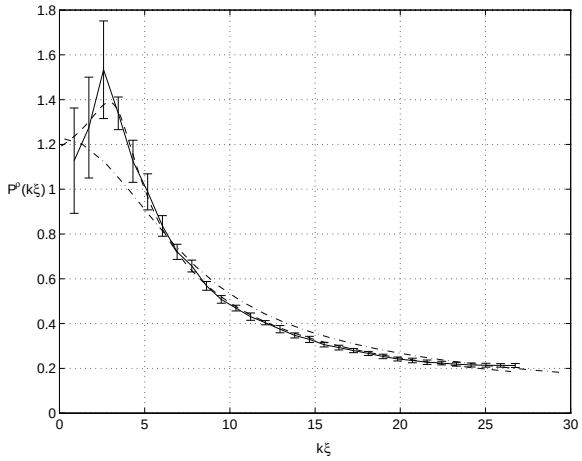

Figure 2: Scaling function for the energy density as defined by equation (8) The solid line is the measured scaling function with $1-\sigma$ error bars from ensemble averaging. The dashed line is the fitted function equation (12). The dash-dot line is the predicted form from our model, the last line in equation (24).

These scaling forms are fixed by the requirement that the density fluctuations obey the scaling law

$$\int_0^{\xi^{-1}} d^3k \, \langle |\Theta_{00}(k,\eta)|^2 \rangle \propto \xi^{-4} \tag{11}$$

with a similar law for the other components of $\Theta_{\mu\nu}$. We display our results for P^ρ, $X^{\rho U}$ and P^U in Figures 2, 3 and 4 along with fits to the following forms

$$P^\rho(z) = \frac{a}{(1-(bz)+(cz)^n)^{1/n}} \tag{12}$$

$$X^{\rho U}(z) = \frac{d}{(1-(ez)+(fz)^m)^{2/m}} \tag{13}$$

$$P^U(z) = \frac{g}{(1-(hz)+(jz)^p)^{0.66/p}} \tag{14}$$

which are motivated by a requirement of white noise at large scales due to uncorrelated initial conditions and good single parameter fits to $P^\rho \sim (k\xi)^{-0.98\pm0.06}$, $P^U \sim (k\xi)^{-0.66\pm0.03}$ and $X^{\rho U} \sim (k\xi)^{-2.0\pm0.1}$ at small scales.

The errors indicate ensemble standard deviation. The other parameters are $a = 1.18$, $b = 0.25$, $c = 0.24$, $n = 6$, $d = 0.23$, $e = 0.3$, $f = 0.5$, $m = 3$, $g = 0.07$, $h = 0.15$, $j = 0.18$ and $p = 1.59$. We consistently get a peak for $P^\rho(z)$ and $P^U(z)$ at $k\xi \simeq 3$ which corresponds to a physical wavelength of about 2ξ. However, it is difficult to be certain about the initial rise in the power spectrum because the error bars are large. In the notation of Magueijo *et al* the peak corresponds to an $x_c = k\eta$ of approximately 20.

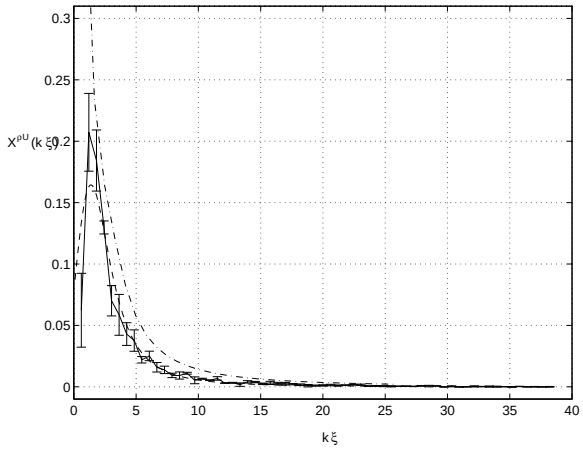

Figure 3: Scaling fucnction for the equal time energy-momentum cross correlator as defined by equation (9). The solid line is the measured scaling function with $1-\sigma$ error bars from ensemble averaging. The dashed line is the fitted function equation (13). The dash-dot line is the predicted form from our model, equation (36).

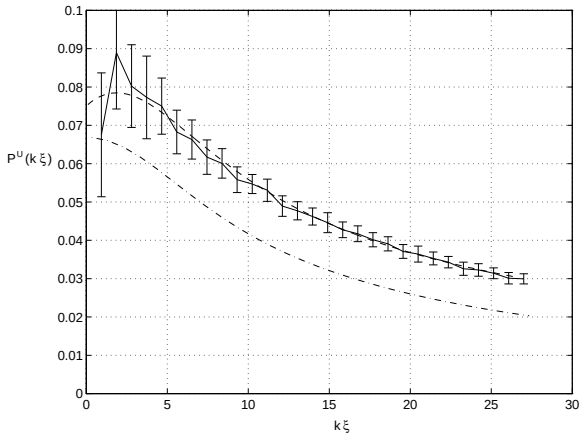

Figure 4: Scaling fucnction for the momentum density as defined by equation (10) The solid line is the measured scaling function with $1-\sigma$ error bars from ensemble averaging. The dashed line is the fitted function equation (14). The dash-dot line is the predicted form from our model, the last line in equation (26).

As discussed above, the real importance of Θ_{00} and Θ_{0i} in the context of perturbation theory is how they are correlated over time. We performed k-space measurements of the two-time correlation functions

$$C^{\rho\rho}(k;\eta,\eta') = V^{-1}\langle\Theta_{00}(k,\eta)\Theta^*_{00}(k,\eta')\rangle \tag{15}$$

$$C^{\rho U}(k;\eta,\eta') = V^{-1}\langle U(k,\eta)\Theta^*_{00}(k,\eta')\rangle \tag{16}$$

$$C^{UU}(k;\eta,\eta') = V^{-1}\langle U(k,\eta)U^*(k,\eta')\rangle \tag{17}$$

During the scaling era they are well approximated by

$$C^{\rho\rho} = \frac{1}{\sqrt{\xi\xi'}}\sqrt{P^\rho(k\xi)P^\rho(k\xi')}\,e^{-\frac{1}{2}\Upsilon^2k^2(1-(k\Delta))(\eta-\eta')^2} \tag{18}$$

$$C^{\rho U} = \frac{1}{\sqrt{\xi\xi'}}\sqrt{P^\rho(k\xi)P^\rho(k\xi')}\,e^{-\frac{1}{2}\Upsilon'^2k^2(\eta-\eta')^2}(\frac{\alpha}{k\sqrt{\xi\xi'}} - \Upsilon'^2k(\eta-\eta')) \tag{19}$$

$$C^{UU} = \frac{1}{\sqrt{\xi\xi'}}\sqrt{P^U(k\xi)P^U(k\xi')}\,e^{-\frac{1}{2}\Upsilon''^2k^2(\eta-\eta')^2}(1-\Upsilon''^2k^2(\eta-\eta')^2) \tag{20}$$

where we have used the scaling forms of the power spectra and cross-correlator and $\xi = \xi(\eta)$, $\xi' = \xi(\eta')$. The imaginary component of these correlators is consistent with zero within the ensemble errors. The forms of these functions are motivated by a model which we describe in the next section.

The values for Υ, Υ' and Υ'' are given in Table 1. Δ is approximately 3δ. These parameters were determined by minimisation of the χ-squared for each realisation. The normal distribution of parameters obtained allows an estimate to be made of each parameter and its $1-\sigma$ errors. We stress that we consider equations (18), (19) and (20) to be an approximation, although a good one for $|\eta-\eta'| \leq 8k^{-1}$. For comparison, the energy and momentum correlators fall to half their maximum value at $|\eta-\eta'| \simeq 3k^{-1}$. Outside the range given there are two effects present in the measured correlators which invalidate the model. The first is small k-dependent oscillations about zero as predicted by Turok [22]. The second is sharp peaks in the correlators at small scales which we take to be an effect of defining strings on the lattice. Figures 5, 6 and 7 show the measured

E_c	Υ	α	Υ'	Υ''
2δ	0.21 ± 0.05	0.19 ± 0.05	0.42 ± 0.05	0.36 ± 0.07
4δ	0.18 ± 0.05	0.16 ± 0.05	0.42 ± 0.05	0.42 ± 0.06

Table 1: Fitted parameters for the models in equations (18), (19) and (20)

functions at a time $\eta' = 22\delta$ (which is within the scaling era of our simulations).

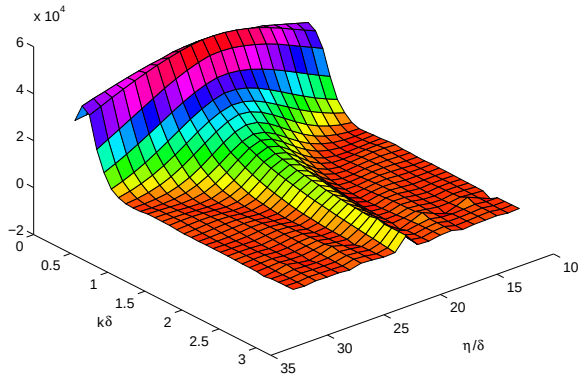

Figure 5: Two-time correlation function $\langle \Theta_{00}(k,\eta)\Theta^*_{00}(k,\eta')\rangle$ for $\eta' = 22\delta$

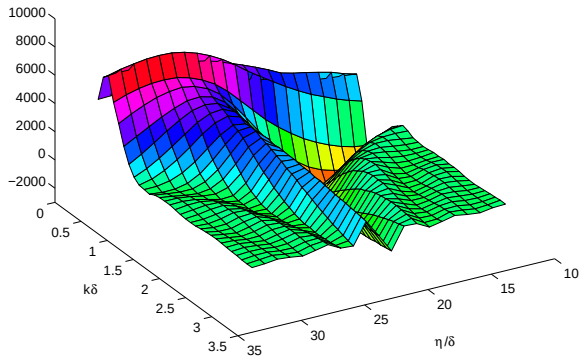

Figure 6: Two-time correlation function $\langle U(k,\eta)\Theta^*_{00}(k,\eta')\rangle$ for $\eta' = 22\delta$

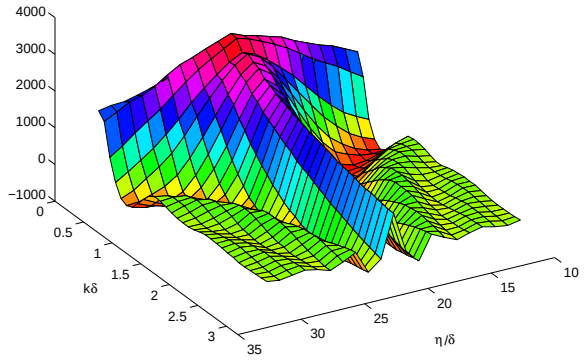

Figure 7: Two-time correlation function $\langle U(k,\eta)U^*(k,\eta')\rangle$ for $\eta' = 22\delta$

From the gaussian fall-off over time we see that for a given mode with wavenumber k the network energy density decorrelates on a characteristic time scale which goes like $1/\Upsilon k\sqrt{(1-(k\Delta))}$ and the momentum density varies as $1/\Upsilon'' k$ for $E_c = 2\delta$.

4 Theoretical Model

4.1 Power Spectra

We can use a very simple model to account for the forms given in (12) and (14), if not the precise details. From (7) we get

$$\Theta^{\mu\nu}(\mathbf{k}) = \int d\sigma\, (\dot{X}^\mu \dot{X}^\nu - X'^\mu X'^\nu) e^{i\mathbf{k}\cdot\mathbf{X}(\sigma,\eta)} \tag{21}$$

At any given time the power spectrum is

$$\langle |\Theta_{00}(k,\eta)|^2 \rangle = \langle \int d\sigma\, d\sigma'\, e^{i\mathbf{k}\cdot(\mathbf{X}(\sigma,\eta)-\mathbf{X}(\sigma',\eta))} \rangle \tag{22}$$

We then make some assumptions about the statistics of the network. Firstly, that for each lag $\sigma_- = \sigma - \sigma'$, the quantities $X_i(\sigma) - X_i(\sigma'), \dot{X}_i(\sigma)$ and $X_i'(\sigma)$ are gaussian random variables with zero mean. Secondly, that the distribution of strings is isotropic. Then

$$\begin{aligned} \langle |\Theta_{00}(k)|^2 \rangle &= \int d\sigma\, d\sigma'\, e^{-\frac{1}{6}k^2 \langle (\mathbf{X}(\sigma)-\mathbf{X}(\sigma'))^2 \rangle} \\ &= \frac{1}{2} \int d\sigma_+\, d\sigma_-\, e^{-\frac{1}{6}k^2\Gamma(\sigma_-)} \end{aligned} \tag{23}$$

where we have introduced the function $\Gamma(\sigma - \sigma') = \langle (\mathbf{X}(\sigma) - \mathbf{X}(\sigma'))^2 \rangle$ and changed variables to $\sigma_- = \sigma - \sigma'$ and $\sigma_+ = \sigma + \sigma'$. We will also use $\bar{t}^2 = \langle \mathbf{X}'^2 \rangle$. The third assumption is that the network is described by a collection of randomly placed string segments of length $\xi/\bar{t}$ and total energy $V\xi^{-2}$, where V is the volume of the simulation box. Then $\Gamma = \bar{t}^2\xi^2(\sigma_-/\xi)^2$ and $L = \frac{1}{2}\int d\sigma_+ = V\xi^{-2}$. If we define $z = \sigma_-\bar{t}/\xi$ then

$$\begin{aligned} \langle |\Theta_{00}(k,\eta)|^2 \rangle &= L \int d\sigma_-\, e^{-\frac{1}{6}k^2\bar{t}^2\xi^2(\sigma_-/\xi)^2} \\ &= \frac{L\xi}{\bar{t}} \int_{-\frac{1}{2}}^{\frac{1}{2}} dz\, e^{-\frac{1}{6}(k\xi)^2 z^2} \\ &= \frac{V}{\xi\bar{t}} \frac{2\sqrt{6}}{k\xi} \mathrm{erf}\left(\frac{k\xi}{2\sqrt{6}}\right) \end{aligned} \tag{24}$$

Thus the scaling form of (8) emerges quite naturally. If we compare (24) with (8), we can write the predicted form of the scaling function $P^\rho(k\xi)$. The large and short wavelength

limits are

$$P^{\rho}(k\xi) = \begin{cases} (k\xi)^0 & \text{if } k\xi << 2\sqrt{6} \\ (k\xi)^{-1} & \text{if } k\xi >> 2\sqrt{6} \end{cases} \tag{25}$$

This function is plotted along with the measured and fitted model in Figure 2. It should be noted that the normalisation is given by the model along with the measurement for $\bar{t}$, and not introduced by hand. This model does better at predicting the measured power spectrum than a random walk model, in which the power on large scales goes like k^{-2}. Therefore, although each individual string is a random walk, they must be highly (anti) correlated on large scales.

Similarly, the power spectrum for U becomes

$$\begin{aligned} \langle |U(k)|^2 \rangle &= \langle \int d\sigma \, d\sigma' \, \hat{k}_i \hat{k}_j \dot{X}^i(\sigma) \dot{X}^j(\sigma') e^{i\mathbf{k}\cdot(\mathbf{X}(\sigma,\eta)-\mathbf{X}(\sigma',\eta))} \rangle \\ &= L \int d\sigma_- \, (\tfrac{1}{3}\mathcal{V}(\sigma_-) - \tfrac{1}{9}k^2\Pi^2(\sigma_-)) e^{-\frac{1}{6}k^2\Gamma(\sigma_-)} \\ &= \frac{2V}{3\xi\bar{t}} \int_0^{\frac{1}{2}} dz \, (\tilde{\mathcal{V}}(z/\bar{t}) - \tfrac{1}{3}(k\xi)^2\tilde{\Pi}^2(z/\bar{t}) e^{-\frac{1}{6}(k\xi)^2 z^2} \end{aligned} \tag{26}$$

where $\mathcal{V}$ and Π are the correlation functions

$$\mathcal{V}(\sigma) = \langle \dot{\mathbf{X}}(\sigma) \cdot \dot{\mathbf{X}}(0) \rangle \tag{27}$$

$$\Pi(\sigma) = \langle \dot{\mathbf{X}}(\sigma) \cdot (\mathbf{X}(\sigma) - \mathbf{X}(0)) \rangle \tag{28}$$

and $\tilde{\mathcal{V}}(\sigma_-/\xi)$ and $\tilde{\Pi}(\sigma_-/\xi)$ are their scaling forms. We have measured these correlation functions elsewhere [19], and we can use them to calculate the scaling function P^U. The result is plotted in Figure 4. Although for very large $k\xi$ this model predicts a $(k\xi)^{-1}$ behaviour, within the k-range of our simulations the model agrees well with our measurements giving a fit to $(k\xi)^{-0.66}$, although the normalisation is not so impressive as for the energy-density.

4.2 Two-time correlation functions

In order to calculate the two-time correlation functions in this framework we need the two-time correlation functions $\Gamma(\sigma, \sigma', \eta, \eta')$, $\mathcal{V}(\sigma, \sigma', \eta, \eta')$ and $\Pi(\sigma, \sigma', \eta, \eta')$. However, we have not yet measured these quantities and instead resort to crude modelling. If we consider small scales we may assume that each segment is moving at a velocity $\bar{v}^2 = \langle \dot{\mathbf{X}}^2 \rangle$ in a random direction orthogonal to the orientation of the segment so that

$$\Gamma(\sigma_-, \eta, \eta') = \bar{t}^2\sigma_-^2 + \bar{v}^2(\eta - \eta')^2 \tag{29}$$

Using equations (24) and (29) we get

$$\langle \Theta_{00}(k,\eta)\Theta^*_{00}(k,\eta')\rangle = \langle |\Theta_{00}(k,\eta)|^2\rangle\, e^{-\frac{1}{6}\bar{v}^2k^2(\eta-\eta')^2} \tag{30}$$

However this model does not reflect the fact that between η and η' some energy is lost and the integrand is no longer independent of $d\sigma_+$. We know that $C^{\rho\rho}(\eta,\eta') = C^{\rho\rho}(\eta',\eta)$ and the most natural way of respecting this condition is to replace the power spectrum at η with the square root of the product of the power spectra at the two times. Hence the final result to be compared with equation (18) is

$$\langle \Theta_{00}(k,\eta)\Theta^*_{00}(k,\eta')\rangle = \frac{1}{\sqrt{\xi\xi'}}\sqrt{P^\rho(k\xi)P^\rho(k\xi')}\; e^{-\frac{1}{6}\bar{v}^2k^2(\eta-\eta')^2} \tag{31}$$

To model the other two-time correlators $\langle U(k,\eta)U^*(k,\eta')\rangle$ and $\langle U(k,\eta)\Theta^*_{00}(k,\eta')\rangle$ we must be careful about the conservation of energy-momentum as loops are created and energy is lost from the long string network. If we assume that the loop production occurs evenly along the string and that we are in a scaling regime we can model in k-space the rate of energy going into loops as

$$\Lambda(k,\eta) = \frac{\lambda(k\xi)}{\xi}\Theta_{00}(k,\eta) \tag{32}$$

The energy-momentum conservation equation becomes

$$U(k,\eta) = \frac{1}{k}\frac{\partial}{\partial\eta}\Theta_{00} + \frac{\lambda}{k\xi}\Theta_{00}(k,\eta) \tag{33}$$

and hence,

$$\begin{aligned}
\langle U(k,\eta)\Theta^*_{00}(k,\eta')\rangle &= \int d\sigma\, d\sigma'\; (\frac{1}{k}\frac{\partial}{\partial\eta} + \frac{\lambda}{k\xi})e^{-\frac{1}{6}k^2(\bar{v}^2(\eta-\eta')^2+\bar{t}^2\sigma_-^2)} \\
&= \int d\sigma\, d\sigma'\; (\frac{\lambda}{k\xi} - \tfrac{1}{3}k\bar{v}^2\eta_-))e^{-\frac{1}{6}k^2(\bar{v}^2(\eta-\eta')^2+\bar{t}^2\sigma_-^2)} \\
&= \langle |\Theta_{00}(k,\eta)|^2\rangle(\frac{\lambda}{k\xi} - \tfrac{1}{3}k\bar{v}^2\eta_-)e^{-\frac{1}{6}\bar{v}^2k^2(\eta-\eta')^2}
\end{aligned} \tag{34}$$

To ensure that we do not pick out a time η we express $C^{\rho U}(\eta,\eta')$

$$\langle U(k,\eta)\Theta^*_{00}(k,\eta')\rangle = \langle \Theta_{00}(k,\eta)\Theta^*_{00}(k,\eta')\rangle\,(\frac{\lambda}{k\sqrt{(\xi\xi')}} - \frac{1}{3}k\bar{v}^2\eta_-) \tag{35}$$

The time dependence of this function is plotted in Figure 8, and should be compared with Figure 9.

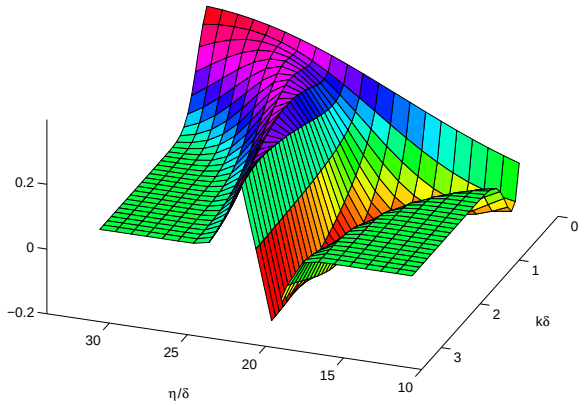

Figure 8: Model of time dependence of $\langle U(k,\eta)\Theta^*_{00}(k,\eta')\rangle$

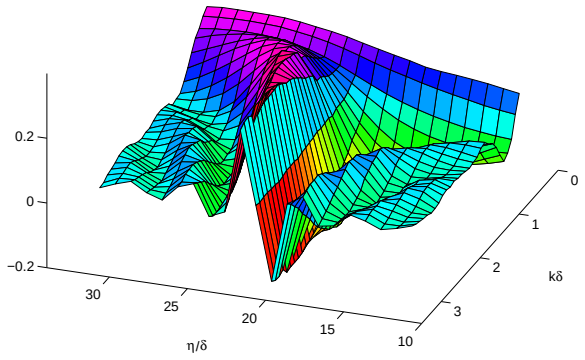

Figure 9: Measured time dependence of $\langle U(k,\eta)\Theta^*_{00}(k,\eta')\rangle$

These plots assume a value of λ measured from the simulations. We find it to be roughly constant at large $k\xi$ at $\lambda \simeq 0.32$ (± 0.03). Including loop production shifts where the cross-correlator goes to zero from $\eta = \eta'$ to $\lambda - \frac{1}{3}k^2\bar{v}^2\eta_-\sqrt{(\xi\xi')} = 0$. The effect of energy loss through loop production on the momentum of the long string may also account for the form of the equal time cross-correlator. If we take $\eta = \eta'$ in equation (35), which in terms of this model gives the correlation between the long string energy and the reaction momentum from loop production, we get

$$X^{\rho U}(k\xi) = \frac{\lambda}{k\xi}P^{\rho}(k\xi) \tag{36}$$

This neatly explains the $(k\xi)^{-2}$ dependence in equation (13), although the measured normalisation is only 60% of that given by the independently measured λ and equation (36). One reason for this discrepancy may be that our model assumes loop production occurs evenly along the string at a constant rate, whereas we observe loop production in more discrete bursts. The prediction from equation (36) is plotted in Figure 3, along with the measured scaling function.

We find that the effect of the loop production term is insignificant for $\langle U(k,\eta)U^*(k,\eta')\rangle$ and we will drop it in the following expression:

$$\begin{aligned}\langle U(k,\eta)U^*(k,\eta')\rangle &= \frac{1}{k^2}\int d\sigma\, d\sigma'\, \frac{\partial}{\partial\eta}\frac{\partial}{\partial\eta'}e^{-\frac{1}{6}k^2(\bar{v}^2(\eta-\eta')^2+\bar{t}^2\sigma_-^2)} \\ &= \langle|\Theta_{00}(k,\eta)|^2\rangle\frac{\bar{v}^2}{3}(1-\frac{\bar{v}^2}{3}k^2(\eta-\eta')^2)e^{-\frac{1}{6}\bar{v}^2k^2(\eta-\eta')^2}\end{aligned} \tag{37}$$

Again to ensure $C^{UU}(\eta,\eta') = C^{UU}(\eta',\eta)$, we use the product of the square root of the power spectra, so that

$$\langle U(k,\eta)U^*(k,\eta')\rangle = \frac{1}{\sqrt{\xi\xi'}}\sqrt{P^{\rho}(k\xi)P^{\rho}(k\xi')}\,\frac{\bar{v}^2}{3}(1-\frac{\bar{v}^2}{3}k^2(\eta-\eta')^2)e^{-\frac{1}{6}\bar{v}^2k^2(\eta-\eta')^2} \tag{38}$$

Equation (38) incorrectly predicts U to have the same $k\xi$ dependence in its power spectrum as the energy, with a relative normalisation given by $\bar{v}^2/3$. We expect a proper treatment in terms of the two-time on-string correlators for Π, $\mathcal{V}$ and Γ to remedy this problem. The time dependence of this function is plotted in Figure 10. As one can verify by comparison with Figure 11, the simplest of assumptions has provided a reasonable approximation to the measured time dependence.

In this section we have motivated the forms in equations (18), (19) and (20). From the model, and using the measurements $\bar{t}^2 = 0.637 \pm 0.010$ and $\bar{v}^2 = 0.363 \pm 0.010$, we can make predictions for the coherence parameters Υ, Υ' and Υ'', and the relative

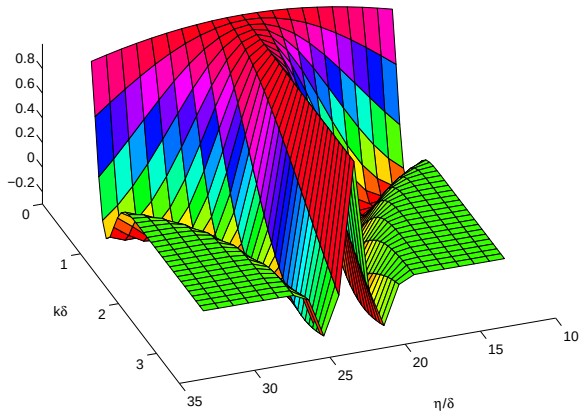

Figure 10: Model of time dependence of $\langle U(k,\eta)U^*(k,\eta')\rangle$

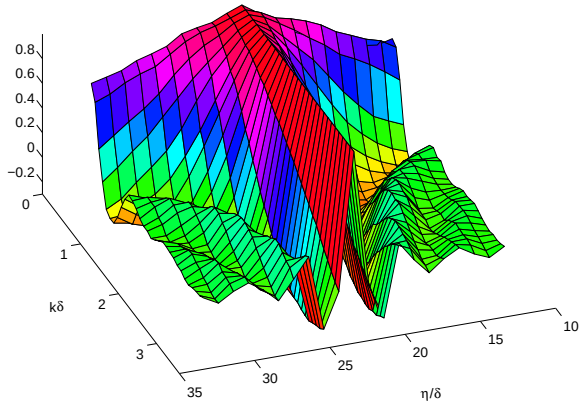

Figure 11: Measured time dependence of $\langle U(k,\eta)U^*(k,\eta')\rangle$

quantity	model	measured
Υ	0.35 ± 0.02	0.21 ± 0.05
Υ'	0.35 ± 0.02	0.42 ± 0.05
Υ''	0.35 ± 0.02	0.36 ± 0.07
R	0.35 ± 0.02	0.38 ± 0.1

Table 2: Parameters for the forms given in equations (18), (19) and (20) as predicted by our model and measured from the simulations. Note a complication in comparing the values of Υ, due to a lattice effect in equation (18) as discussed in the text.

normalisation $R = \langle \Theta_{00}(k,\eta)\Theta^*_{00}(k,\eta')\rangle / \langle U(k,\eta)U^*(k,\eta')\rangle$. The measured values are for $E_c = 2\delta$. The comparison for Υ is complicated by an apparent lattice effect accounted for in equation (18) by the length scale Δ. We assume that as Δ goes to zero and the form in equation (18) approaches that in equation (31), allowing a comparison to be made. Not surprisingly, the model is not wholly satisfactory. We know that the momentum density does not have the same $(k\xi)$ dependence as the energy density, which is predicted by (38). Also from (18) we see that the strings decorrelate on a time scale $\sim 1/k\sqrt{(1-(k\Delta))}$ and not k^{-1}. One might think that both features are understandable as it is well known that strings move faster on smaller scales. This gives faster decorrelation and greater power in the momentum density on small scales than the simple model would suggest. Having said this, we note that the scale Δ introduced in equation (18) is close to the lattice scale and is fairly constant throughout the simulation. Consequently, the departure from a k^{-1} coherence time may be due to the fact that the strings are defined at all times on the lattice. It is puzzling that this effect does not show up in the other correlators. Furthermore, the model does not account for the oscillations about zero in the two-time correlators. The oscillations are present in all three two-time correlators, but are most obvious in Figures 9 and 11. As Turok has recently pointed out [22], such oscillations should appear in the Fourier transforms of two-time spatial correlators because of a causality constraint which sets the correlator to zero for causally disconnected points.

5 Conclusions

We have demonstrated the scaling properties of the power spectra and cross correlator of two important energy-momentum quantities, the density Θ_{00} and the velocity U, and given the large k behaviour. We have also studied the two-time correlators and measured the time coherence in the network.

We find that the energy and the momentum power spectra are peaked at around $k\xi \simeq 3$, where $\xi \simeq 0.15\eta$, thereafter decaying as $(k\xi)^{-1}$ and $(k\xi)^{-0.66}$ respectively over the range of our simulations. The cross-correlator decays as $(k\xi)^{-2}$ and is peaked at $k\xi \simeq 2$.

For a mode of spatial frequency k, the two-time correlation functions of Θ_{00} and U display correlations over time scales of $\eta_c \simeq 4.7k^{-1}$ and $\eta_c \simeq 2.4k^{-1}$ respectively. The time scale η_c^2 is the variance in the Gaussian fall-off as a function of the time difference (see equations (18) and (20)). We have presented simple models to explain the qualitative results, predicting the power spectra and cross correlator including normalisations, to a reasonable accuracy, and accounted for the features of the two-time correlation functions.

The model describes the string network as a set of randomly placed segments of length $\xi/\bar{t}$, where $\bar{t} = (1 - \bar{v}^2)^{\frac{1}{2}}$, with random velocities. We assume that relevant quantities such as velocities and extensions between points with a given separation in σ are gaussian random variables. We can then reduce ensemble averaging to the study of two-point correlations along the string, which we must model or measure.

From the model we can show that the characteristic coherence time scale for a mode of spatial frequency k is $\eta_c \simeq 3/k$. Our simulations give a similar result, although at very small scales η_c decrease faster than k^{-1}. This we believe to be a lattice effect.

There are potential pitfalls in taking the Minkowski space string network as a source for the fluid perturbation variables in a Friedmann model. For example, the energy conservation equation is modified to

$$\dot{\Theta}_{00} + \frac{\dot{a}}{a}(\Theta_{00} + \Theta) - kU = -\Lambda \tag{39}$$

where $a(\eta)$ is the scale factor and $\Theta = \Theta_{ii}$ the trace of the spatial components of $\Theta_{\mu\nu}$. Since Θ is unconstrained by any conservation equation, its fluctuations could drive a fluctuating component in Θ_{00} whose time scale would go like $a/\dot{a}$ [23]. However, we find that $\langle|\Theta|^2\rangle << \langle|\Theta_{00}|^2\rangle$ and believe the introduction of the $\dot{a}/a$ term to be a small effect.

If we take the simulations at face value, the implications for the appearance of the Doppler peaks are not entirely clear cut. The coherence time is smaller than, but of the same order of magnitude as, the period of acoustic oscillations in the photon baryon fluid at decoupling, which is roughly $11/k$ [24]. This is in turn smaller than the time at which the power in the energy and velocity sources peak, approximately $20/k$. The computations of Magueijo *et al* [8] of the Microwave Background angular power spectrum for various source models suggest small or absent secondary peaks. However, our string correlation functions can be used as realistic sources to settle the issue.

Acknowledgements

We wish to thank Andy Albrecht, Nuno Antunes, Pedro Ferreira, Paul Saffin and Albert Stebbins for useful discussions.

GRV and MBH are supported by PPARC, by studentship number 94313367, Advanced Fellowship number B/93/AF/1642 and grant number GR/K55967. MS is supported by the Tomalla Foundation. Partial support is also obtained from the European Commission under the Human Capital and Mobility programme, contract no. CHRX-CT94-0423.

References

[1] A. Vilenkin and E.P.S. Shellard, *Cosmic Strings and other Topological Defects* (Cambridge University Press, Cambridge, 1994)

[2] M. Hindmarsh and T. Kibble *Rep. Prog. Phys* **58** 477 (1994)

[3] S. Veeraraghavan and A. Stebbins *Ap. J.* **365**, 37 (1990)

[4] D. Austin, E. J. Copeland and T. W. B. Kibble *Phys. Rev.* **D48**, 5594 (1993)

[5] M. Hindmarsh SUSX-TH-96-005 `hep-th/9605332` (unpublished)

[6] W. Hu, D. N. Spergel and M. White `astro-ph 9605193`

[7] J. Magueijo, A. Albrecht, D. Coulson and P. Ferreira *Phys. Rev. Lett.* **76** 2617 (1996)

[8] J. Magueijo, A. Albrecht, D. Coulson and P. Ferreira *MRAO-1917* `astro-ph/9605047`

[9] R. Durrer, A. Gangui and M. Sakellariadou *Phys. Rev. Lett.* **76** 579 (1996)

[10] R. G. Crittenden and N. Turok *Phys. Rev. Lett.* **75**, 2642 (1995)

[11] A. Albrecht, D. Coulson, P. Ferreira and J. Magueijo *Phys. Rev. Lett.* **76** 1413 (1996)

[12] E. J. Copeland, T. W. B. Kibble and D. Austin *Phys. Rev.* **D45** (1992)

[13] A. Albrecht and N. Turok *Phys. Rev.* **D40**, 973 (1989)

[14] D. P. Bennett, in "Formation and Evolution of Cosmic Strings", eds. G. Gibbons, S. Hawking and T. Vachaspati, (Cambridge University Press, Cambridge. 1990); F. R. Bouchet *ibid.*; E. P. S. Shellard and B. Allen *ibid.*;

[15] M. Sakellariadou and A. Vilenkin *Phys. Rev.* **D37**, 885 (1988)

[16] M. Sakellariadou and A. Vilenkin *Phys. Rev.* **D42**, 349 (1990)

[17] T. Vachaspati and A. Vilenkin *Phys. Rev.* **D30**, 2036 (1984)

[18] A.G. Smith and A. Vilenkin *Phys. Rev.* **D36**, 990 (1987)

[19] M. Hindmarsh, M.Sakellariadou and G. Vincent (in preparation)

[20] M. Hindmarsh *Ap. J.* **431**, 534 (1994)

[21] M. Hindmarsh *Nucl. Phys. B (Proc. Suppl.)* **43**, 50 (1995)

[22] N. Turok `astro-ph/9604172` (1996)

[23] A. Stebbins, private communication (1996)

[24] P. J. E. Peebles *The Large Scale Structure of the Universe* (Princeton University Press, Princeton, 1980)